

Asymmetric bifunctional protein nanoparticles through redesign of self-assembly

Santiago Sosa^{1,2}, Andrés H. Rossi¹, Alan M. Szalai², Sebastián Klinke^{1,3}, Jimena Rinaldi¹, Ana, Farias¹, Paula M. Berguer¹, Alejandro D. Nadra⁴, Fernando D. Stefani^{2,5}, Fernando A. Goldbaum^{1,3}, Hernán R. Bonomi^{1,&,#}

¹Fundación Instituto Leloir, IIBBA-CONICET, Av. Patricias Argentinas 435, (C1405BWE) Ciudad Autónoma de Buenos Aires, Argentina.

²Centro de Investigaciones en Bionanociencias (CIBION)-CONICET, Godoy Cruz 2390 (C1425FQD), Ciudad Autónoma de Buenos Aires, Argentina.

³Plataforma Argentina de Biología Estructural y Metabolómica PLABEM, Av. Patricias Argentinas 435 (C1405BWE) Ciudad Autónoma de Buenos Aires, Argentina.

⁴Departamento de Fisiología, Biología Molecular y Celular, Departamento de Química Biológica and IQUIBICEN-CONICET, Facultad de Ciencias Exactas y Naturales, Universidad de Buenos Aires, Ciudad Universitaria, Pabellón 2 (C1428EHA), Ciudad Autónoma de Buenos Aires, Argentina.

⁵Departamento de Física, Facultad de Ciencias Exactas y Naturales, Universidad de Buenos Aires, Pabellón 1 Ciudad Universitaria (C1428EHA), Ciudad Autónoma de Buenos Aires, Argentina

[&]Current address: Centre de Biochimie Structurale, CNRS UMR5048, INSERM U1054, Université de Montpellier, 29 rue de Navacelles (34090), Montpellier, France.

#To whom correspondence should be addressed: hbonomi@leloir.org.ar

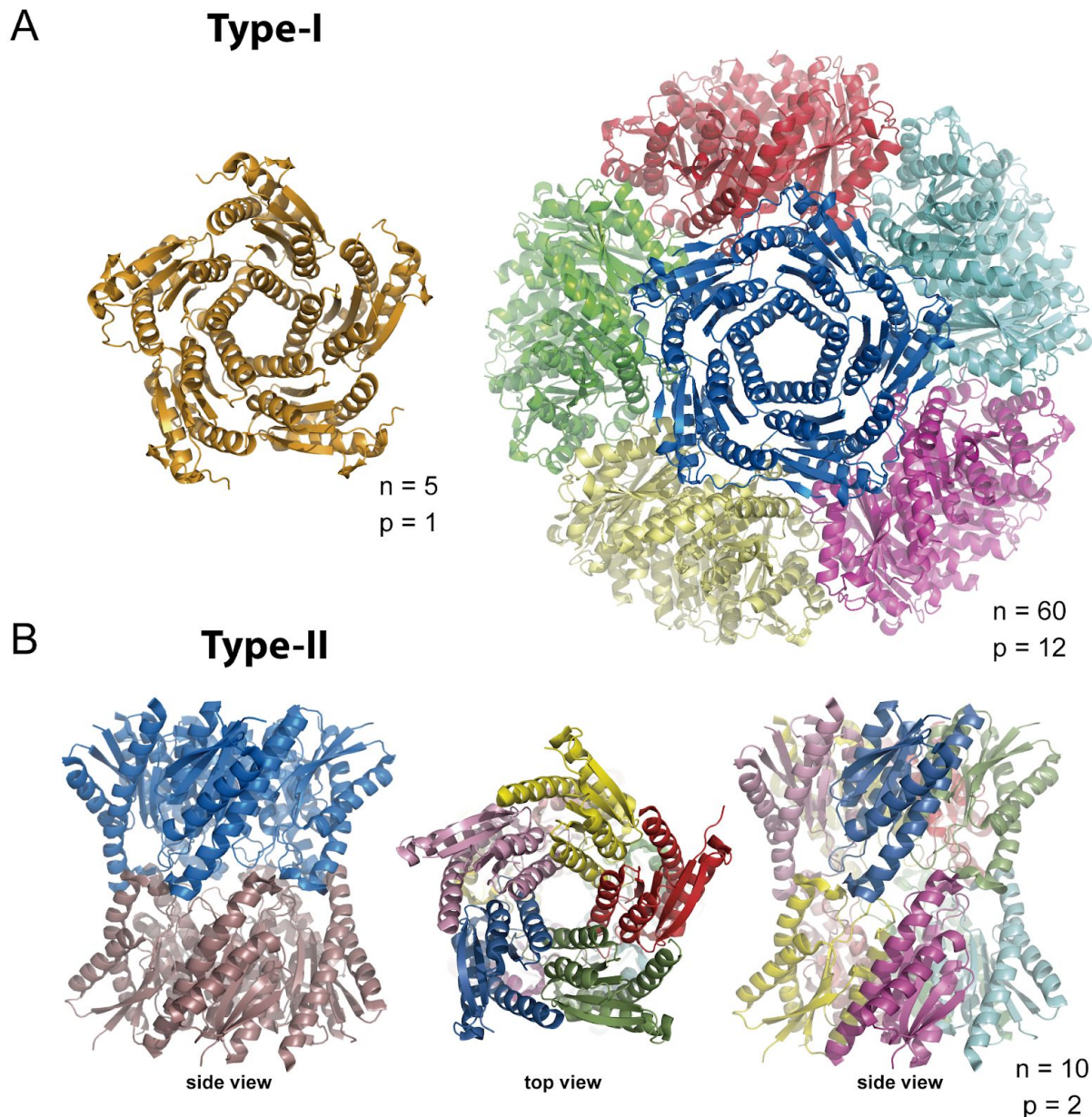


Figure S1. Quaternary arrangements of Lumazine Synthases.

Different examples of (A) Type-I and (B) Type-II LSs in cartoon representation. The number of monomers (n) and the number of pentamers (p) per particle are indicated. Pentamers are shown in different colors except when indicated. (A) Pentameric LS from *Schizosaccharomyces pombe* (PDB 1KYV)¹ and icosahedral LS from *Bacillus subtilis* (PDB 1RVV)². (B) Decameric LS from *Brucella abortus* (PDB 1XN1)³. Center and right panels: monomers are shown in different colors.

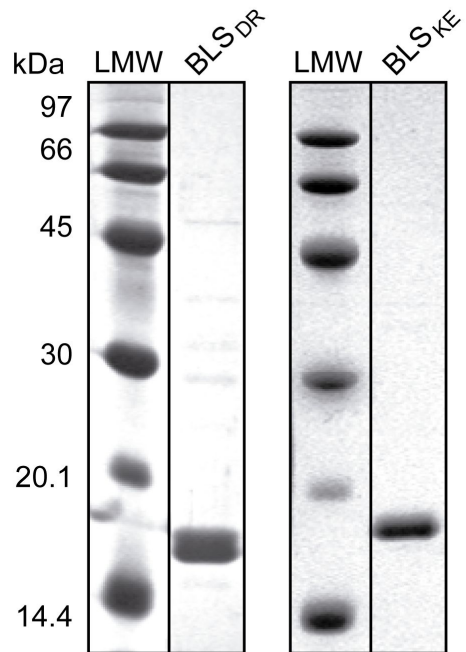


Figure S2. Purity evaluation of BLS_{DR} and BLS_{KE} proteins.

Protein preparations were analyzed by SDS-PAGE and stained with Coomassie blue after the size exclusion chromatography purification step.

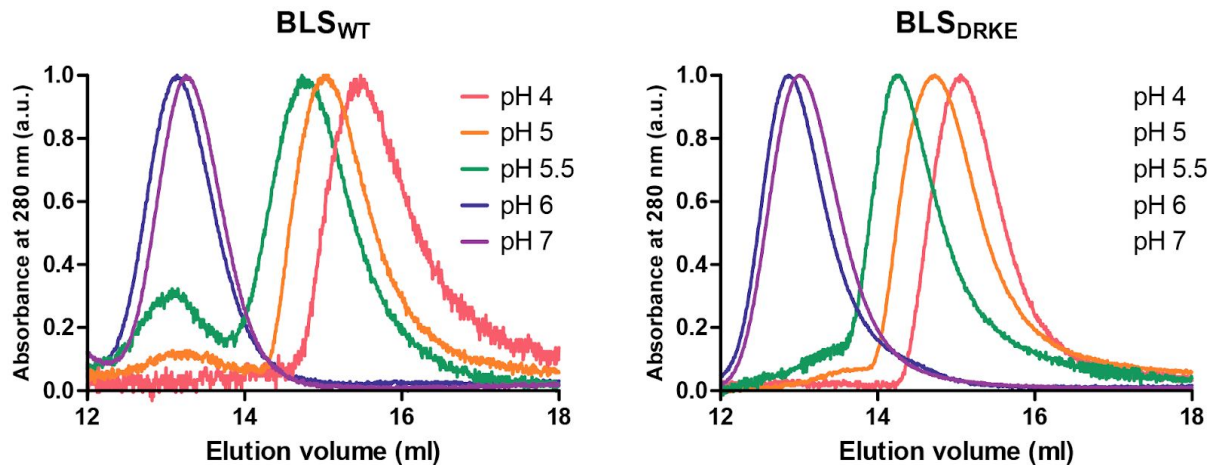


Figure S3. Pentamer-pentamer interaction dependence on the pH value.

BLS_{WT} and BLS_{DRKE} decamer dissociation curves at pH 4-7. The data presented correspond to SEC-SLS measurements at each pH value. The MW was calculated for each peak and pentamer:decamer proportions estimated at each pH value for both proteins used in **Figure 4D** using a two-gaussian fitting.

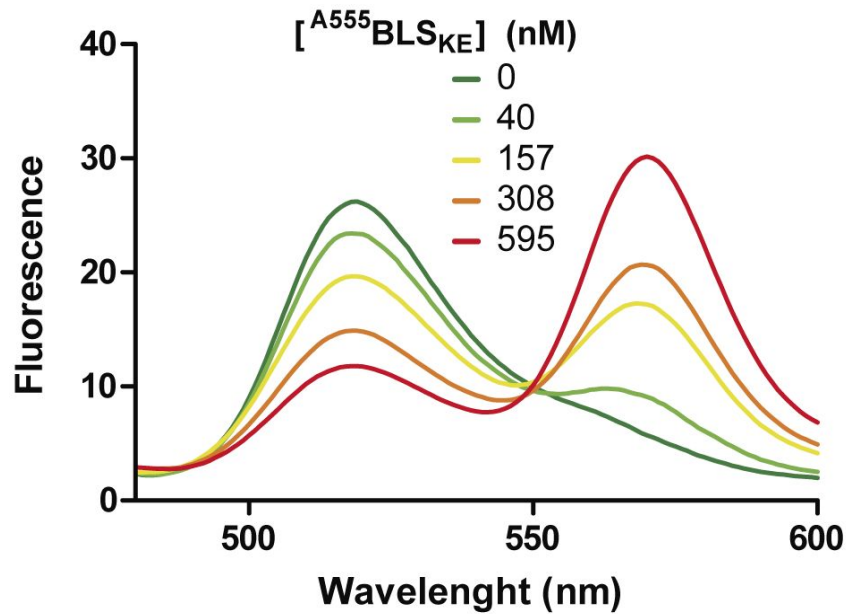


Figure S4. FRET effect between fluorescent BLS_{DR} and BLS_{KE} pentamers.

Fluorescence spectra (λ_{exc} : 470 nm) of 15 nM ${}^{\text{A}488}\text{BLS}_{\text{DR}}$ incubated with increasing ${}^{\text{A}555}\text{BLS}_{\text{KE}}$ concentrations.

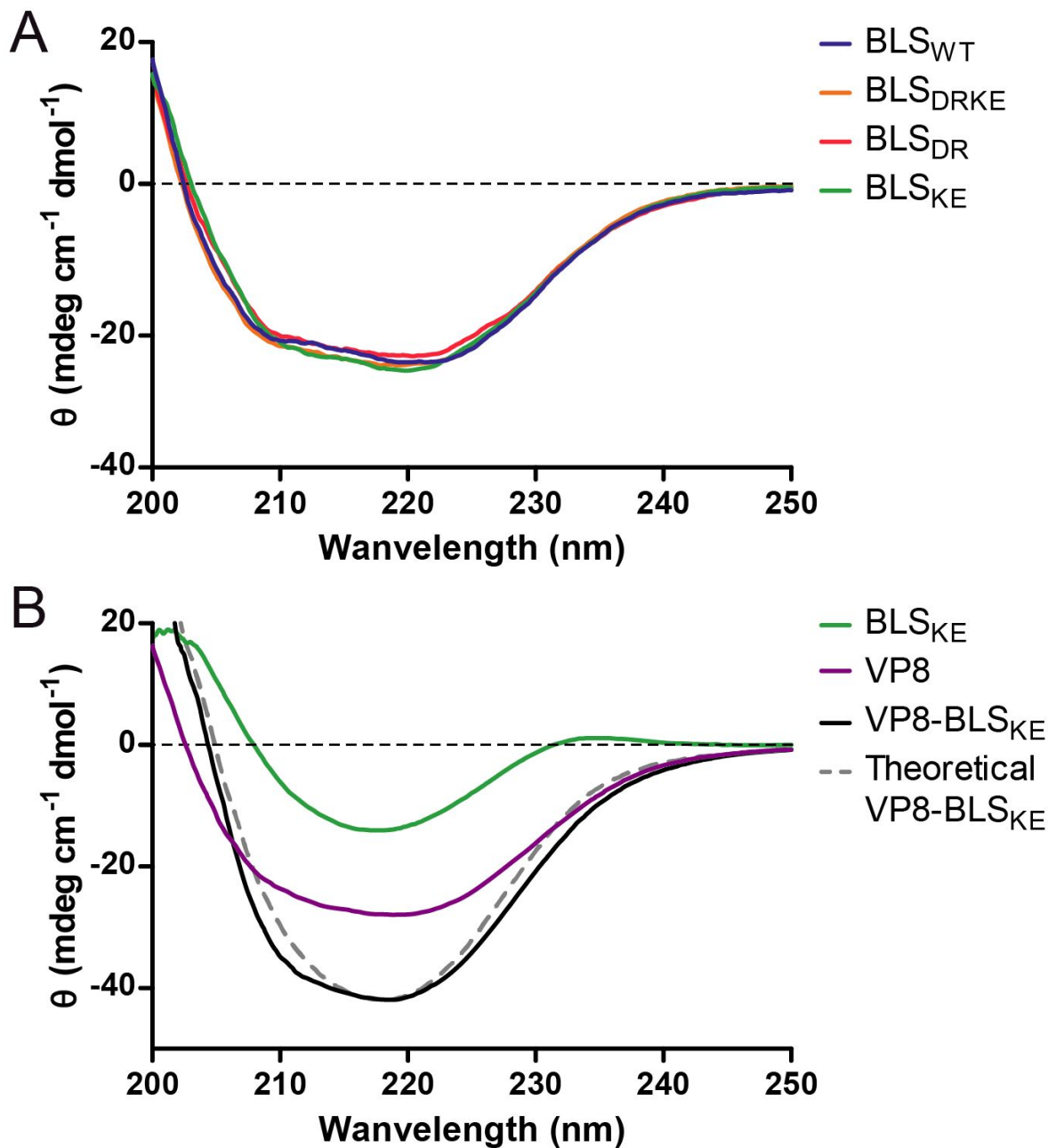


Figure S5. Far-UV circular dichroism of BLS decameric and pentameric versions.

Mean ellipticity spectra of A) BLS_{WT}, BLS_{DR}, BLS_{KE} and BLS_{DRKE}, and B) BLS_{KE}, VP8 and VP8-BLS_{KE}, measured at 25 °C, pH 7.8. The theoretical VP8-BLS_{KE} spectrum was calculated as the sum of VP8 and BLS_{KE} spectra.

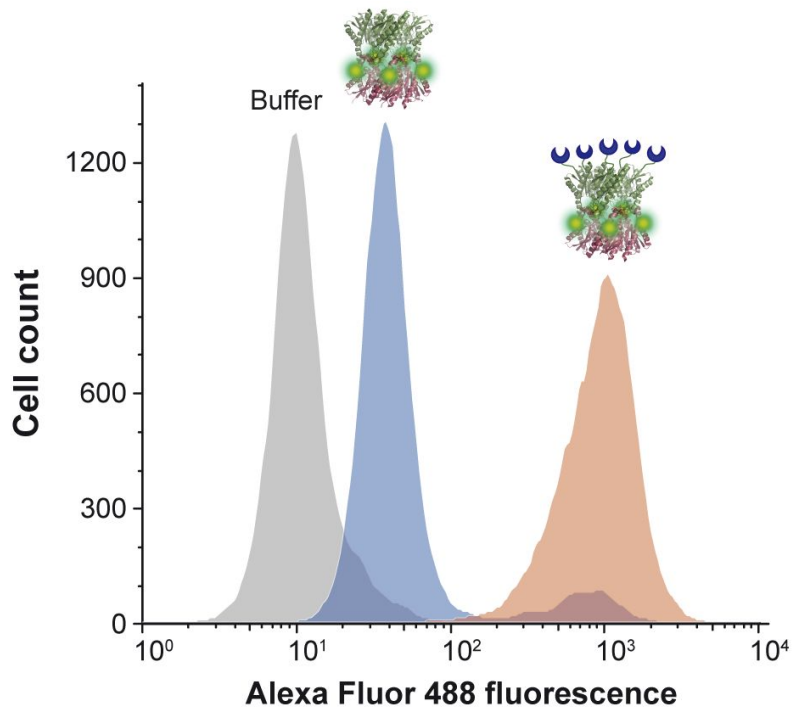


Figure S6. Flow cytometry of non-adherent cells labeled with a bifunctionalized BLS_{DRKE}.

Flow cytometry fluorescence histograms of NS0 murine cells incubated with PBS buffer (grey) and $^{A488}\text{BLS}_{\text{DR}}$ with BLS_{KE} (blue) or VP8-BLS_{KE} (orange), both proteins at 50 mg/ml.

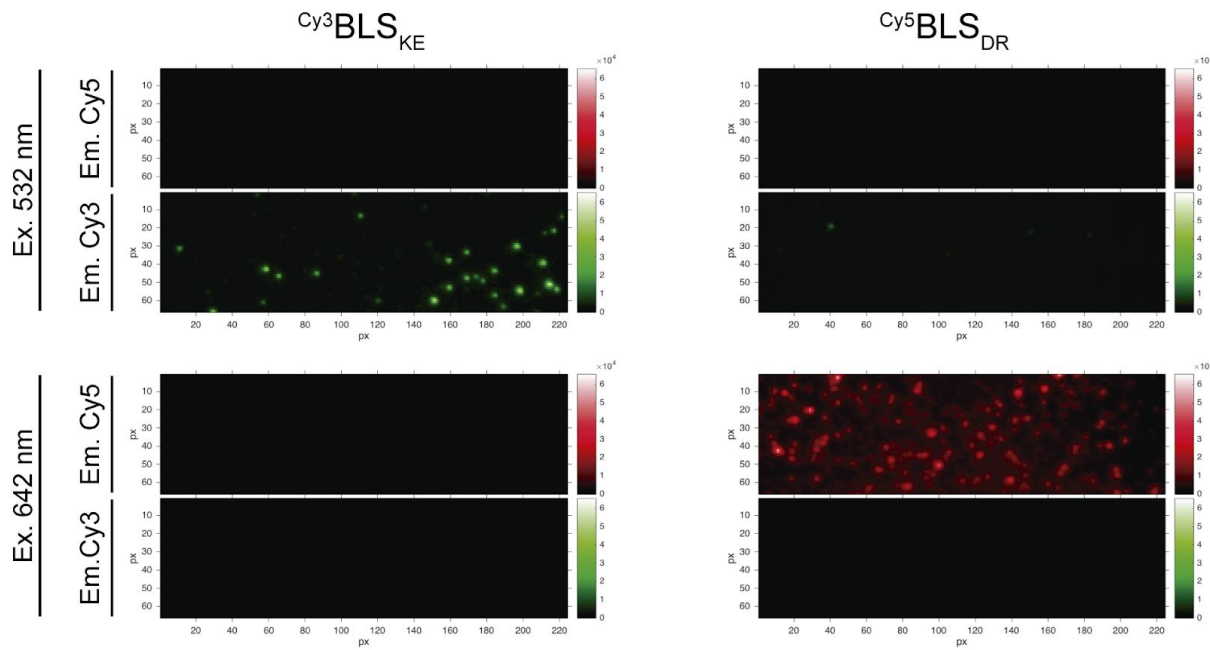


Figure S7. Wide-field two-color epifluorescence TIRF microscopy of $\text{Cy}^5\text{BLS}_{\text{KE}}$ and $\text{Cy}^3\text{BLS}_{\text{DR}}$ particles. Between 100 and 500 cumulative images were acquired using emission filters for Cy3 and Cy5. Pixel values were relativized to the maximum value for each emission channel, subtracting their respective minimum values, rescaled to [0-65535], and represented by the colormap scales.

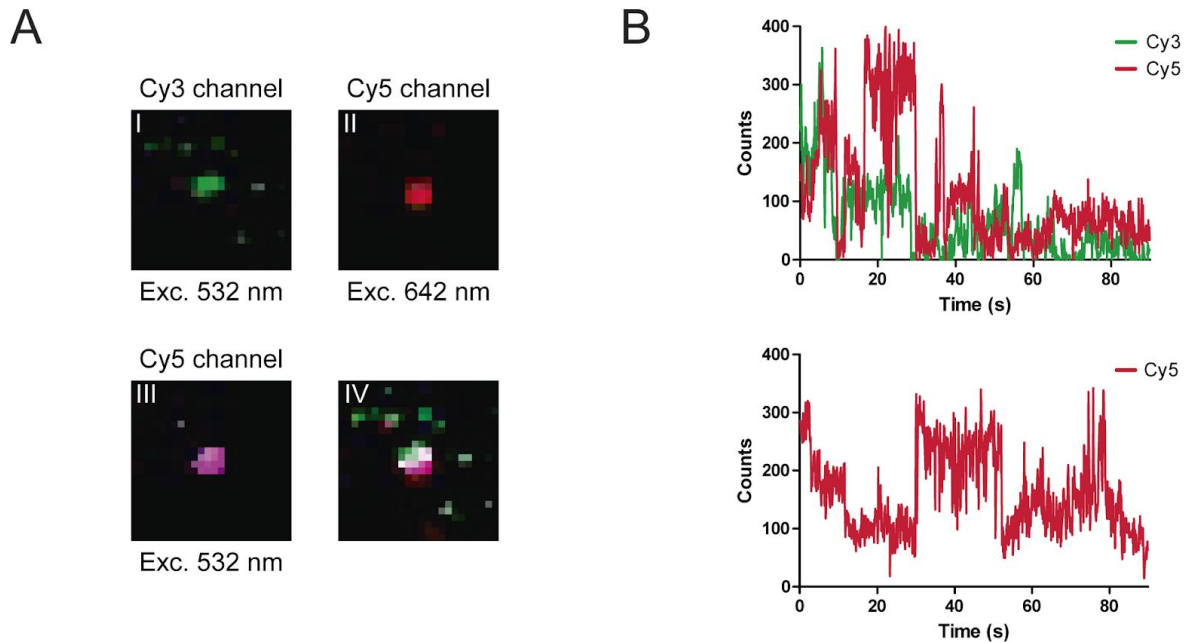


Figure S8. Example of smFRET of co-localizing $\text{Cy}^5\text{BLS}_{\text{KE}}$ and $\text{Cy}^3\text{BLS}_{\text{DR}}$ particles.

(A) Images derived from TIRF microscopy of pre-incubated $\text{Cy}^5\text{BLS}_{\text{KE}}$ and $\text{Cy}^3\text{BLS}_{\text{DR}}$. Excitation lasers: 532 nm (panels I and III) and 642 nm (panel II); emission filters: Cy3 (panel I) and Cy5 (panels II and III). Panel IV is a merge of images from panels I and II. Each image represents a 90-s acquisition interval. (B) 90-s fluorescence time traces derived from the spot shown in (A). Top panel: Cy3 and Cy5 channels excited with a 532 nm laser. Bottom panel: Cy5 channel excited with a 642 nm laser.

Table S1. Primers and plasmids used in this study.

Primer	Sequence (5'-3')	Characteristics / mutation	References
BLS_C5S_F	caaagctctccgaacaagacat	C5S	This work
BLS_C5S_R	tgttcggagagcttggttcaa	C5S	This work
BLS_DD_F	gtcgtgtgacgcggacactccatgaaagcaag	H117D/H118D	This work
BLS_DD_R	cttgcttcatgaaagtgcgtccggcgatcacgac	H117D/H118D	This work
BLS_RR_F	agcaaggagcataccgcatttccatgccattcaaggtaag	D127R/A131R	This work
BLS_RR_R	cttcacattgaaatggcgatgaaagaagcggtatgctccttgc	D127R/A131R	This work
BLS_KK_F	gtcgtgtgacgcgaagaagtccatgaaagcaag	H117K/H118K	This work
BLS_KK_R	cttgcttcatgaaacttccatggcgatcacgac	H117K/H118K	This work
BLS_EE_F	agcaaggagcatacgaatttccatgaacattcaaggtaag	D127E/A131E	This work
BLS_EE_R	cttcacattgaaatgttcatgaaatccatggcgatgctccttgc	D127E/A131E	This work
BLS_DR-K123C_F	gacgactccatgaaagctgtgagcataccgc	K123C	This work
BLS_DR-K123C_R	gaagcggtgatgctcacagcttcatgaaatgc	K123C	This work
BLS_KE-K123C_F	aagaagtccatgaaagctgtgagcatacgaaatc	K123C	This work
BLS_KE-K123C_R	gaattcgtgatgctcacagcttcatgaaacttctt	K123C	This work
VP8-BLS_F	ttgtttaacttaagaaggagata <u>catatg</u> catgaaaccagtgc ttgatggaccatatac	pET11a-VP8d sequences. NdeI restriction site: <u>catatg</u> .	This work
VP8-BLS_R	aaggatgt <u>cattaa</u> gaccgctaccgctacctaattttatgc tattcagtgcatttgc	AflII restriction site: <u>cattaa</u> . Designed to anneal at BLS residue number 5	This work
Plasmid	Template derived from / Primers used	Characteristics / mutations	References
pBLS _{WT}	pET11a-BLS	BLS with wild-type interface. Contains C5S mutation to avoid the use of reducing agents to impair aggregation	This work
pBLS _D	pBLS _{WT} / BLS_DD_F-BLS_DD_R	H117D/H118D	This work
pBLS _{DR}	pBLS _D / BLS_RR_F-BLS_RR_R	H117D/H118D/D127R/A131R	This work
pBLS _K	pBLS _{WT} / BLS_KK_F-BLS_KK_R	H117K/H118K	This work
pBLS _{KE}	pBLS _K / BLS_EE_F-BLS_EE_R	H117K/H118K/D127E/A131E	This work
pBLS _{DR-C}	pBLS _{DR} / BLS_DR-K123C_F-BLS_DR-K123C_R	H117D/H118D/D127R/A131R/K123C	This work
pBLS _{KE-C}	pBLS _{KE} / BLS_KE-K123C_F-BLS_KE-K123C_R	H117K/H118K/D127E/A131E/K123C	This work
pVP8-BLS	pET11a-BLS	N-terminal VP8d GSGSG-BLS	¹
pVP8-BLS _{KE}	pBLS _{KE} / VP8-BLS_F-VP8-BLS_R	N-terminal VP8d GSGSG-BLS _{KE}	This work

Table S2. Gibbs free energy between pentamers for BLS variants calculated with FoldX.

BLS variant	ΔG_{pp} (kCal/mol)	Relative ΔG_{pp}
BLS _{WT}	-23,35 ± 1,60	1,00 ± 0,14
D81A	-16,36 ± 0,57	0,70 ± 0,10
I84A	-17,98 ± 0,88	0,77 ± 0,12
H117A	-23,13 ± 0,44	0,99 ± 0,09
H118A	-20,94 ± 0,72	0,90 ± 0,10
H117A+H118A	-13,38 ± 0,81	0,57 ± 0,13
H120A	-27,45 ± 1,95	1,18 ± 0,13
E124A	-16,44 ± 0,43	0,70 ± 0,09
H125A	-18,68 ± 0,79	0,80 ± 0,11
F128A	-9,88 ± 0,50	0,42 ± 0,12
H132A	-14,33 ± 0,23	0,61 ± 0,08
E124A+H132A	-14,08 ± 0,39	0,60 ± 0,10
E124A+F128A+H132A	-2,32 ± 0,25	0,10 ± 0,18

BLS protein sequences.

Mutations are colored in blue, red, yellow and green. VP8 is highlighted in light grey and the linker region in dark grey.

>BLS-WT (C5S)

```
MNQSSPNKTSFKIAFIQARWHADIVDEARKSFVAELAAKTGGSVEVEIFDVPGAYEIPLHAKTLART
GRYAAIVGAAFVIDGGIYRHDVFATAVINGMMQVQLETEVPVL SVVLTPHHFHE SKEHHDF HAHFK
VKGV EA AHA ALQIV SERSRIAALV
```

>BLS-DR

```
MNQSSPNKTSFKIAFIQARWHADIVDEARKSFVAELAAKTGGSVEVEIFDVPGAYEIPLHAKTLART
GRYAAIVGAAFVIDGGIYRHDVFATAVINGMMQVQLETEVPVL SVVLTP DD FHE SKEHH RFF HRF K
VKGV EA AHA ALQIV SERSRIAALV
```

>BLS-KE

```
MNQSSPNKTSFKIAFIQARWHADIVDEARKSFVAELAAKTGGSVEVEIFDVPGAYEIPLHAKTLART
GRYAAIVGAAFVIDGGIYRHDVFATAVINGMMQVQLETEVPVL SVVLTP KK FHE SKEHH E FF HE HFK
VKGV EA AHA ALQIV SERSRIAALV
```

>VP8-BLS-KE

```
MHEPVLDGPYQPTTFNPPVS YWMILLAP TNAGVVAEGTNNTNRWLATILIEPNVQQVERTYTLFGQQ
VQVT VSND SQT KWK FVD LSK QT QDG NYSQ HGPLL STPK LYGV MKH GRIY TYN GET PNATT GYY ST
TNFD TVNMT AYCDF YI I PLA QEA KCT EY INN GLGSG SGL KTS FKIAFIQARWHADIVDEARKSFVA
ELAA KTG GSVE VE IFD VPG AYE IP L HAK TLART GRYAAIVGAAFVIDGGIYRHDVFATAVINGMMQ
VQLE TEVP VL SVVL TP KK FHE SKEHH E FF HE HF KVKG VEA AHA ALQIV SERSRIAALV
```

>BLS-DR-K123C

```
MNQSSPNKTSFKIAFIQARWHADIVDEARKSFVAELAAKTGGSVEVEIFDVPGAYEIPLHAKTLART
GRYAAIVGAAFVIDGGIYRHDVFATAVINGMMQVQLETEVPVL SVVLTP DD FHE SCE HH RFF HRF K
VKGV EA AHA ALQIV SERSRIAALV
```

>BLS-KE-K123C

```
MNQSSPNKTSFKIAFIQARWHADIVDEARKSFVAELAAKTGGSVEVEIFDVPGAYEIPLHAKTLART
GRYAAIVGAAFVIDGGIYRHDVFATAVINGMMQVQLETEVPVL SVVLTP KK FHE SCE HH E FF HE HF K
VKGV EA AHA ALQIV SERSRIAALV
```

Supplementary References

- 1 D. Bellido, P. O. Craig, M. V. Mozgovoj, D. D. Gonzalez, A. Wigdorovitz, F. A. Goldbaum and M. J. Dus Santos, *Vaccine*, 2009, **27**, 136–145.